ELSEVIER

Signal Processing 77 (1999) 49–62

SIGNAL PROCESSING

www.elsevier.nl/locate/sigpro

DOA and frequency estimation using fast subspace algorithms

Mohammed A. Hasan*

Department of Electrical and Computer Engineering, University of Minnesota Duluth, Duluth, MN 55812, USA

Received 3 October 1996; received in revised form 5 January 1999

Abstract

Eigendecomposition-based methods such as MUSIC, minimum norm, and ESPRIT estimators are popular for their high resolution property in sinusoidal and direction of arrival (DOA) estimation but they are also known to be of high computational demand. In this paper, new fast and robust algorithms for DOA frequency estimation are presented. These algorithms approximate the required signal and noise subspace using rational and power-like methods applied to the sample covariance matrix and have been shown to be applicable to ESPRIT-type as well as MUSIC-type methods. It is also shown that a substantial computational saving would be gained compared to those associated with the eigendecomposition-based methods. Simulations results show that these approximated estimators have comparable performance at low signal-to-noise ratio (SNR) to their standard counterparts and are robust against overestimating the number of impinging signals. © 1999 Published by Elsevier Science B.V. All rights reserved.

Zusammenfassung

Methoden, die auf einer Eigenzerlegung beruhen – wie zum Beispiel MUSIC, Minimum-Norm und ESPRIT Schätzer-, sind für die Schätzung von Sinussignalen und von Einfallsrichtungen (DOA) wegen ihrer hohen Auflösung beliebt, aber sie sind auch für ihren hohen Bedarf an Rechenleistung bekannt. In dieser Arbeit werden neue schnelle und robuste Algorithmen für die DOA Frequenzschätzung vorgestellt. Diese Algorithmen approximieren die benötigten Signal- und Geräuschunterräume unter Verwendung von rationalen und potenzartigen Methoden, die auf die empirische Kovarianzmatrix angewendet werden, und von ihnen wurde gezeigt, daß sie sowohl auf Methoden vom ESPRIT-Typ als auch vom MUSIC-Typ anwendbar sind. Es wird dargelegt, daß eine substantielle Verringerung des Rechenaufwands erzielt würde, wenn man mit jenem der auf Eigenzerlegungen basierenden Methoden vergleicht. Simulationsergebnisse lassen erkennen, daß diese approximierten Schätzer bei geringem Signal-Geräuschabstand (SNR) vergleichbare Leistung aufweisen wie ihre Standard-Pendants und daß sie robust gegenüber einer Überschätzung der Anzahl einfallender Signale sind. © 1999 Published by Elsevier Science B.V. All rights reserved.

Résumé

Les méthodes basées sur la décomposition propre telles que les estimateurs MUSIC, à norme minimale, et ESPRIT, sont populaires du fait de leur haute résolution pour l'estimation des sinusoïdes et des directions d'arrivée (DOA) mais elles sont aussi connues pour leur charges de calcul importantes. Des algorithmes rapides et robustes nouveaux pour l'estimation de DOA sont présentés dans cet article. Ces algorithmes approximent le sous-espace signal et bruit requis à l'aide de méthodes rationnelles et de type puissance appliquées à la matrice de covariance et sont montrés être applicables aux méthodes de type ESPRIT et MUSIC. Il est montré que des économies en calcul substantielles seraient

*E-mail: mhasan@u.mn.edu

PII: S0165-1684(99)00022-5

obtenues vis-à-vis des méthodes basées sur la décomposition propre. Les résultats de simulation montrent que les estimateurs approximés ont des performances semblables à rapport signal sur bruit (SNR) faible et sont robustes vis-à-vis de la sur-estimation du nombre de signaux arrivant.

Keywords: MUSIC; Minimum Norm; ESPRIT; DOA; Frequency estimation; Power methods; Rational subspace approximation

1. Introduction

Estimation of sinusoidal frequencies and DOA embedded in white noise is a problem of interest in many fields of signal processing such as geophysics, radar and sonar. Several high-resolution techniques emerged during the last few years for solving this problem. For useful articles and books in this area, the reader is referred to [14] and the references therein. Generally, modern high resolution sub-space estimation schemes are of three types: (i) extrema searching techniques like spectral MUSIC [21], (ii) polynomial rooting techniques such as Root-MUSIC [18] and Pisarenko methods [14], and (iii) matrix shifting methods such as ESPRIT [9,17,19,20], matrix pencils and unitary ESPRIT [9,11]. There has been a growing research activity for improving the performance of high-resolution eigenstructure methods with the goal of lowering the SNR resolution threshold or lowering their computational load. A class of methods based on the eigenstructure of the covariance matrix of the data has received a particular attention, using one or both subspaces. Among the well known singular value decomposition (SVD)-based methods are MUSIC, Minimum Norm and ESPRIT. These methods and their statistical efficiency are studied in [3,10,13,22,24]. In these methods, the autocorrelation matrix of large order (usually much bigger than the number of sinusoids to provide a more accurate modeling of the noise) obtained from the data is decomposed and the signal and noise vectors are extracted according to the relative magnitudes of the singular values. However, these methods are computationally demanding since they involve the computation of each singular eigenvector and corresponding eigenvalue. In high-resolution methods such as MUSIC, Minimum Norm and ESPRIT, the noise and/or signal subspace are all that needed rather than the individual singular vectors. To reduce the computational cost associated with these methods, various alternatives were proposed by several authors. In [15], Kay and Shaw suggested the use of polynomials and rational functions of the sample covariance matrix for approximating the signal subspace. In [23], Tufts and Melissinos used Lanczos and power-type method to approximate the signal subspace. Karhunen and Joutsenalo [12] approximated the signal subspace using the discrete Fourier and Cosine transforms. Ermolaev and Gershman [4] used powers of sample covariance matrix based on Krylov subspaces to approximate the noise subspace when the number of impinging signals and a threshold which separates the signal and noise eigenvalues are known a priori. However, in most applications these parameters are unknown and thus place a serious limitation on the usefulness of these techniques. These methods have shown significant computational saving over those which explicitly compute eigen or singular vectors, however, none of these methods are developed in the context of the less costly ESPRIT method. Therefore, the objective of this paper is to extend the results of [4,12,15,23] in approximating the signal and noise subspaces and apply them for the derivation of ESPRIT-type as well as MUSIC-type methods. This include a method of estimating signal subspace when the number of sources are known and no a priori knowledge of a threshold is required. This is an improvement of the method in [4] where both the number of sources and the threshold must be known. The approach presented here is also useful in other DOA estimators such as beamspace MUSIC [2], FINE [16] and generalized MIN-NORM [6].

This paper is organized as follows. Section 2 describes the data model of the frequency estimation problem and the problem formulation. The estimation of sample covariance matrix is presented in Section 3. Approximated subspace estimators based on rational and power approximations are given in Sections 4 and 5. Operation count is discussed in Section 6. Finally, simulation results are provided in Section 7, followed by a conclusion in Section 8.

2. Problem formulation

Consider a linear array of p sensors and q multiple narrow-band signals impinging on the array with DOA angles $\theta_1, \theta_2, \dots, \theta_q$. Assuming that p snapshots are available, the received signal at the array can be expressed as

$$\boldsymbol{x}(k) = A(\theta)\boldsymbol{s}(k) + \boldsymbol{v}(k), \tag{1a}$$

where $\boldsymbol{s}(k) \in \mathscr{C}^q$ ($\mathscr{C}$ is the field of complex numbers) is a vector of complex signals of q wavefronts

$$\boldsymbol{s}(k) = [s_1(k) \quad s_2(k) \quad \dots \quad s_q(k)]^{\mathrm{T}}, \tag{1b}$$

$\boldsymbol{v}(k)$ is a $p \times 1$ vector of additive noise in sensors with

$$\boldsymbol{v}(k) = [v_1(k) \quad v_2(k) \quad \dots \quad v_p(k)]^{\mathrm{T}}, \tag{1c}$$

and A is a $p \times q$ matrix

$$A(\theta) = [\boldsymbol{a}(\theta_1) \quad \boldsymbol{a}(\theta_2) \quad \dots \quad \boldsymbol{a}(\theta_q)], \tag{1d}$$

with $\boldsymbol{a}(\theta) = [1 \ \mathrm{e}^{\mathrm{j}w(\theta)} \ \mathrm{e}^{\mathrm{j}2w(\theta)} \ \dots \ \mathrm{e}^{\mathrm{j}(p-1)w(\theta)}]^{\mathrm{T}}$ being the steering vector of the array toward the direction θ. Here $w(\theta)$ is some known function which is solvable for θ. It is also assumed that the signals and additive noise are zero-mean stationary complex-valued random processes such that $\mathrm{E}[v_i(k)v_j^*(k)] = \sigma_v^2\delta_{i-j}$ for $i, j = 1, \dots, p$, where σ_v^2 is the variance of v. Here $E[\cdot]$ and $*$ denote the expectation and conjugate transpose operators, respectively. The spatial $p \times p$ covariance matrix of the array output is given by $R_x := \mathrm{E}[\boldsymbol{x}(k)\boldsymbol{x}^*(k)] = A(\theta)R_sA(\theta)^* + \sigma_v^2 I_p$ with $R_s = \mathrm{E}[\boldsymbol{s}(k)\boldsymbol{s}^*(k)]$ is $q \times q$ covariance matrix of $\boldsymbol{s}$ and I_p is the $p \times p$ identity matrix. Note that the minimum eigenvalue of R_x is equal to σ_v^2 with multiplicity $p - q$. If the θs are all distinct, the unknown matrix $A \in \mathscr{C}^{p \times q}$ is of rank q. The main objective is to estimate q and the directions of arrival of the sources from p snapshots of the array A from the noisy data $\{x(k)\}_{k=1}^N$.

3. Computation of the sample covariance matrix

In the sequel, $\hat{R}_x$ will denote the sample covariance matrix while R_x will denote the true covariance matrix. To effectively use the structure of the data, the correlation matrix R_x is estimated using the forward-backward method so that $\hat{R}_x = \frac{1}{2(N-p+1)} X_p^* X_p$, where

$$X_p = \left[\begin{array}{cccc} x(p) & x(p-1) & \cdots & x(1) \\ x(p+1) & x(p) & \cdots & x(2) \\ \cdots & \cdots & \cdots & \cdots \\ x(N) & x(N-1) & \cdots & x(N-p+1) \\ \hdashline x(1)^* & x(2)^* & \cdots & x(p)^* \\ x(2)^* & x(3)^* & \cdots & x(p+1)^* \\ \cdots & \cdots & \cdots & \cdots \\ x(N-p+1)^* & x(N-p+2)^* & \cdots & x(N)^* \end{array}\right]. \tag{2}$$

It is known that the theoretical covariance matrix is Toeplitz and centro-symmetric, i.e., $R_x = JR_x^*J$, where J is the permutation matrix with ones along the cross diagonal. Thus one may expect that the forward-backward method in Eq. (2) yields a better estimate of R_x than if it is estimated using only the lower or upper part of X_p.

In the SVD-based methods, the correlation matrix R_x is decomposed as $R_x = U_1\Lambda_1V_1^* + U_2\Lambda_2V_2^*$, where $U_i^*U_j = \delta_{i-j}I_p$, $V_i^*V_j = \delta_{i-j}I_p$, $U_i^*V_j = 0$ and Λ_i is a diagonal matrix for $i, j = 1, 2$. Here δ_{i-j} denotes the Kronecker delta function, Λ_1 represents the diagonal matrix of the most significant singular values and Λ_2 is a diagonal matrix whose diagonal holds the least significant singular values. Several techniques are available in the literature to compute the SVD or to solve the eigenvalue problem in general. Well-established methods can be found in EISPACK [5,8]. The computational complexity of these algorithms is of order $\mathrm{O}(p^3)$, where p is the size of the matrix. In the subsequent sections we utilize the idea that for high SNR, signal singular values are generally larger than noise singular values and thus powering would widen the separation of the noise and signal eigenvectors.

It is known [25] that the sample and true covariance matrices satisfy $\hat{r}_x(m) = r_x(m) + O(1/\sqrt{N})$, where $r_x(m) = E\{x(k)x^*(k+m)\}$. Thus $\hat{R}_x = R_x + O(1/\sqrt{N})$. The additive term $O(1/\sqrt{N})$ decreases to zero in probability as $N \to \infty$. It can be shown [8] that $\lambda_i = \hat{\lambda}_i + O(1/\sqrt{N})$ where $\{\lambda_i\}_{i=1}^p$ and $\{\hat{\lambda}_i\}_{i=1}^p$ are the sets of eigenvalues of R_x and $\hat{R}_x$, respectively. Therefore, any of the methods applied here using sample covariance matrices yields consistent estimates of the amplitudes and frequencies.

4. Rational approximation of signal subspace

Since the covariance matrix R_x is Hermitian, it has the eigendecomposition $R_x = \sum_{i=1}^p \lambda_i \boldsymbol{u}_i \boldsymbol{u}_i^*$, where λ_i and $\boldsymbol{u}_i$ are the ith eigenvalue and ith corresponding eigenvector. For convenience, it is assumed that the eigenvalues are sorted in decreasing order so that $\lambda_1 \geqslant \lambda_2 \ldots \geqslant \lambda_q > \lambda_{q+1} = \cdots = \lambda_p = \sigma_v^2$ and that the corresponding eigenvectors $\{\boldsymbol{u}_i\}_{i=1}^p$ satisfy $\boldsymbol{u}_i^* \boldsymbol{u}_j = \delta(i-j)$. The eigenvectors $\{\boldsymbol{u}_i\}_{i=1}^q$ are usually called the signal vectors which span the signal subspace with projection $U_s U_s^* = \sum_{i=1}^q \boldsymbol{u}_i \boldsymbol{u}_i^*$ and the eigenvectors $\{\boldsymbol{u}_i\}_{i=p+1}^p$ are called the noise vectors which span the noise subspace with projection $U_n U_n^* = \sum_{i=q+1}^q \boldsymbol{u}_i \boldsymbol{u}_i^*$. When the noise $v(k)$ is white process, $A(\theta) R_s A^*(\theta) = U_s \Lambda^2 U_s^*$, where $\Lambda^2 = \mathrm{diag}(\lambda_1, \lambda_2, \ldots, \lambda_q)$ and hence $A(\theta) R_s^{1/2} = U_s \Lambda V$ for some unitary matrix V. Therefore, $U_n^* A(\theta) R_s^{1/2} = U_n^* U_s \Lambda V = 0$ from which it follows $U_n^* A(\theta_i) = 0$ or equivalently $\{\boldsymbol{u}_i\}_{i=q+1}^p$ are orthogonal to $\{\boldsymbol{a}(\theta_i)\}_{i=1}^q$. The signal subspace is spanned by the vectors $\{\boldsymbol{a}(\theta_i)\}_{i=1}^q$ and thus the last relation simply means that $\{\boldsymbol{u}_i\}_{i=q+1}^p$ span the noise subspace.

In [4], an algorithm which computes an approximation of the noise subspace basis is derived using rational functions. This algorithm required a priori knowledge of the number of impinging signals and a threshold λ_{thr} which separates signal and noise eigenvalues. The approximated noise subspace was then given by $\{(R_x^m/\lambda_{\mathrm{thr}}^m) + I_p\}^{-1}$ for sufficiently large value of m. Using this approximation, the minimum norm solution [4] was derived. However, no procedure was provided for choosing λ_{thr}. It was shown through simulations that a rough estimate of λ_{thr} can be obtained from the equation

$$\lambda_{\mathrm{thr}} \approx \frac{\mathrm{Tr}(R_x)}{p} \tag{3}$$

provided that p is sufficiently large. Here $\mathrm{Tr}(B)$ denotes the trace of A which is the sum of the diagonal entries of B. One can see the validity of this equation from noting that $\lambda_i \geqslant \sigma_v$ for $1 \leqslant i \leqslant p$ and hence $\mathrm{Tr}(R_x) = \sum_{i=1}^p \lambda_i \geqslant p\sigma_v$. In the next theorem, we generalize the above idea to obtain a rational approximation of the signal subspace.

Theorem 1. *Let $R_x = \sum_{i=1}^p \lambda_i \boldsymbol{u}_i \boldsymbol{u}_i^*$, where λ_i and $\boldsymbol{u}_i$ are the ith eigenvalue and corresponding eigenvector, Let $b \geqslant 0$ such that $\lambda_1 \geqslant \lambda_2 \cdots \geqslant \lambda_q > b > \lambda_{q+1} = \cdots = \lambda_p = \sigma_v^2$ with corresponding eigenvectors $\{\boldsymbol{u}_i\}_{i=1}^p$. Let $U_s = [\boldsymbol{u}_1 \quad \boldsymbol{u}_2 \quad \ldots \quad \boldsymbol{u}_q]$ and $U_n = [\boldsymbol{u}_{q+1} \quad \boldsymbol{u}_{q+2} \quad \ldots \quad \boldsymbol{u}_p]$, then*
1. *$F_m^{(1)} = (b^m I_p - \hat{R}_x^m)(b^m I_p + \hat{R}_x^m)^{-1}$ converges to $U := U_n U_n^* - U_s U_s^*$ as $m \to \infty$. (Note that $U_s U_s^* = (I_p - U)/2$ and $U_n U_n^* = (I_p + U)/2$).*
2. *$F_m^{(2)} = \hat{R}_x^m (b^m I_p + \hat{R}_x^m)^{-1}$ converges to $U_s U_s^*$ as $m \to \infty$.*
3. *$F_m^{(3)} = b^m (b^m I_p + \hat{R}_x^m)^{-1}$ converges to $U_n U_n^*$ as $m \to \infty$.*

Proof. See Appendix A. □

In the next few subsections we apply Theorem 1 to obtain approximate minimum norm, MUSIC and ESPRIT estimators.

4.1. An approximated minimum norm algorithm

The minimum norm solution of the DOA problem as formulated in [6,12] is to find $\boldsymbol{w} \in \mathscr{C}^p$ which solves the minimization problem

$$\text{Minimize } \boldsymbol{w}^* \boldsymbol{w} \text{ subject to } U_s^* \boldsymbol{w} = 0 \text{ and } \boldsymbol{W}^{\mathrm{T}} \boldsymbol{e}_1 = 1, \tag{4}$$

where $\boldsymbol{e}_1$ is the first column of the $p \times p$ identity matrix and U_s is the projection of the signal subspace. Then, the minimum norm estimator determines the q highest peaks of the function $P_{\mathrm{MN}}(\theta)$ given by

$$P_{\mathrm{MN}}(\theta)=\frac{1}{|\boldsymbol{a}^*(\theta)U_nU_n^*\boldsymbol{e}_1|^2}. \tag{5a}$$

Note that the vector $\boldsymbol{e}_1$ in Eq. (5a) can be replaced by any vector $\boldsymbol{c}$ that is not in the signal subspace with $\boldsymbol{c}^*\boldsymbol{e}_1\neq 0$ to obtain

$$P_{\mathrm{MN}}(\theta)=\frac{1}{|\boldsymbol{a}^*(\theta)U_nU_n^*\boldsymbol{c}|^2}. \tag{5b}$$

Thus by approximating $U_nU_n^*$ as in Theorem 1, we obtain

$$P_{\mathrm{MN}}^{(m,i)}(\theta)=\frac{1}{|\boldsymbol{a}^*(\theta)(I_p-G_m^{(i)})\boldsymbol{e}_1|^2},\quad i=1,2,3, \tag{6}$$

where $G_m^{(i)}$ for $i=1,2,3$ is an estimate of the signal subspace obtained from Part 1, 2 or 3 of Theorem 1. Clearly $P_{\mathrm{MN}}^{(m,i)}(\theta)$ converges to $P_{\mathrm{MN}}(\theta)$ as $m\to\infty$.

4.2. An approximated MUSIC

The standard MUSIC is defined as

$$P_{\mathrm{MUSIC}}(\theta)=\frac{1}{|\boldsymbol{a}^*(\theta)(I_p-U_sU_s^*)\boldsymbol{a}(\theta)|}=\frac{1}{|p-\boldsymbol{a}^*(\theta)U_s-U_s^*\boldsymbol{a}(\theta)|},$$

where the frequencies are estimated as the locations of the peaks of $P_{\mathrm{MUSIC}}(\theta)$. The signal subspace approximations of Theorem 1 yield the following approximated MUSIC estimators:

$$P_{b,\mathrm{MUSIC}}^{(m,i)}(\theta)=\frac{1}{|p-\boldsymbol{a}^*(\theta)G_m^{(i)}\boldsymbol{a}(\theta)|},\quad i=1,2,3. \tag{7}$$

By applying Theorem 1, we conclude that $P_{b,\mathrm{MUSIC}}^{(m,i)}(\theta)$ converges to $P_{\mathrm{MUSIC}}(\theta)$ for $i=1,2,3$. Note that this estimator is dependent on the parameter b. An approximated threshold b can be provided as in the following algorithm.

Algorithm 1. (Rational-MUSIC)

1. Choose $m\geqslant 1$ for sufficiently large m and compute
$$F_m^{(1)}=\left(\left(\frac{\mathrm{Tr}(\hat{R}_x)}{p}\right)^m I_p-\hat{R}_x^m\right)\times\left(\left(\frac{\mathrm{Tr}(\hat{R}_x)}{p}\right)^m I_p+\hat{R}_x^m\right)^{-1}$$
and let $\bar{F}_m=\frac{1}{2}(F_m^{(1)}+F_m^{(1)*})$.
2. Compute the approximated noise subspace $\hat{U}_n\hat{U}_n^*=(I_p+\bar{F}_m)/2$.
3. Compute $P_{b,\mathrm{MUSIC}}^{(m)}(\theta)$ using $P_{b,\mathrm{MUSIC}}^{(m)}(\theta)=1/|\boldsymbol{a}^*(\theta)(\hat{U}_n\hat{U}_n^*a(\theta)|$ and locate the peaks. The frequencies are estimated as the angular positions of the peaks.

4.3. An approximated rational-ESPRIT

The computional cost associated with the search of the peaks of MUSIC-type algorithms is usually very demanding particularly for large dimensions. Several methods were proposed in the literature to lower the computational requirements of the traditional subspace methods such as ESPRIT, Unitary-ESPRIT and Root-MUSIC. In these methods, the computation is focused on estimating the frequencies by solving an eigenvalue problem or a polynomial rather than searching the whole plane or a circle. Then the frequencies are estimated as the angular positions of the eigenvalues of a matrix formed from the powers of the sample correlation matrix. Normally, each of the MUSIC, Root-MUSIC and minimum norm estimators requires the estimation of the noise subspace, while ESPRIT-type methods require the knowledge of the signal subspace. The main idea behind ESPRIT can be explained as follows. Let $A(\theta)$ be as defined in Eqs. (1a)–(1d), then the signal subspace is the column space of $A(\theta)$. Generally $A(\theta)$ is unknown, however, a basis of the signal subspace can be obtained from the most significant eigenvectors of the correlation matrix. It can easily be shown that $E_2A(\theta)=E_1A(\theta)S$, where $E_i\in\hat{R}^{p-1\times p}$ with E_1 is the identity matrix with the last row removed, while E_2 is the identity matrix with the first row removed and $S=\mathrm{diag}(z_1,z_2,\ldots,z_q)$, where $z_i=\mathrm{e}^{\mathrm{j}w(\theta_i)}$. Hence, $(E_1A(\theta))^+E_2A(\theta)=S$. Here B^+ denotes the generalized inverse of B. This property also holds for any matrix Q whose column space is the signal subspace in which case $Q = A(\theta)P$ for some non-singular matrix P. In this case, if $Q_i = E_iQ$, $i = 1, 2$, then $Q_1^+ Q_2 = P^{-1}(E_1 A(\theta))^+ E_2 A(\theta) P = P^{-1} S P$, which is similar to S. To develop an ESPRIT-type method based on the rational approximation of the noise and signal subspaces given in Theorem 1, let b be a threshold separating the noise and signal eigenvalues, then from the above discussion it can be shown that

$$\lim_{m\to\infty} (E_1 \hat{R}_x^m (b^m I_p + \hat{R}_x^m)^{-1})^+ E_2 \hat{R}_x^m (b^m I_p + \hat{R}_x^m)^{-1} = P_1^{-1} S P_1, \tag{8}$$

for some non-singular matrix P_1. Thus the directions of arrival can be estimated from the eigenvalues of the matrix of the left hand side of Eq. (8) for large m. Simulations showed that $m = 4$ normally produced reasonable results.

5. Power-like methods

In this section, we derive an approximation of the signal subspace using only powers of $\hat{R}_x$. As shown next if the number q is known, then the signal subspace can be approximated to any desired degree of accuracy.

Theorem 2. *Let U_s be as defined in Theorem 1, and let $E_q \in \mathscr{C}^{p\times 1}$ be a matrix such that $E_q^* U_s$ is nonsingular. Define $\hat{R}_q^{(M)} = \hat{R}_x^m E_q$ and set $Q_m = \hat{R}_q^{(m)} (\hat{R}_q^{(m)} * \hat{R}_q^{(m)})^{-1} \hat{R}_q^{(m)*}$. Then Q_m converges to $U_s U_s^*$ as $m \to \infty$, where $U_s U_s^*$ is the projection onto the signal subspace.*

Proof. See Appendix B. □

Theorem 2 can be considered as a basis of many subspace algorithms as shown in Section 5.1.

5.1. Power-like estimators

Let $\hat{R}_Q^{(m)}$ be as in Theorem 2, then a second approximated MUSIC may be given by

$$P_{\mathrm{MUSIC}}^{(m)}(\theta) = \frac{1}{|\boldsymbol{a}^*(\theta)(I_p - \hat{R}_q^{(m)}(\hat{R}_q^{(m)*}\hat{R}_q^{(m)})^{-1}\hat{R}_q^{(m)*})\boldsymbol{a}(\theta)|}, \tag{9}$$

and one can show that

$$\lim_{m\to\infty} P_{\mathrm{MUSIC}}^{(m)}(\theta) = P_{\mathrm{MUSIC}}(\theta).$$

Similarly, the minimum norm estimator can be written as

$$P_{\mathrm{MN}}^{(m)}(\theta) = \frac{1}{|\boldsymbol{a}^*(\theta)(I_p - \hat{R}_q^{(m)}(\hat{R}_q^{(m)*}\hat{R}_q^{(m)})^{-1}\hat{R}_q^{(m)*})\boldsymbol{e}_1|}, \tag{10}$$

which converges to $P_{\mathrm{MN}}(\theta)$ given in Eq. (5a).

Practically, the matrix E_q in the last result can be replaced with any $p \times q$ full rank matrix whose columns share some components of U_s, i.e., $E_q^{\mathrm{T}} U_s$ is full rank. A more efficient method which can be viewed as a modification of Theorem 2 is presented in the following MUSIC algorithm. Note that this algorithm requires a rough estimate of the number of sources.

Algorithm 2. (Power-MUSIC)

1. Choose m sufficiently large and let $\hat{R}_x^m = [\boldsymbol{c}_1^{(m)} \ \boldsymbol{c}_2^{(m)} \ \ldots \ \boldsymbol{c}_p^{(m)}]$, where $\boldsymbol{c}_i^{(m)}$ is the ith column of $\hat{R}_x^m$.
2. Choose the q columns of largest magnitudes and form the matrix $C_q^{(m)} = [\boldsymbol{c}_{i_1}^{(m)} \ \boldsymbol{c}_{i_2}^{(m)} \ \ldots \ \boldsymbol{c}_{i_q}^{(m)}]$ with $\|\boldsymbol{c}_{i_1}\| \geqslant \|\boldsymbol{c}_{i_2}\| \geqslant \ldots \geqslant \|\boldsymbol{c}_{i_q}\| > \|\boldsymbol{c}_{i_r}\|$, $r = q+1, \ldots, p$.
3. Compute $Q_q^{(m)} = C_q^{(m)}(C_q^{(m)*}C_q^{(m)})^{-1}C_q^{(m)*}$.
4. Plot $P_{\mathrm{MUSIC}}^{(m)}(\theta) = 1/(p - \boldsymbol{a}^*(\theta) Q_q^{(m)} Q_q^{(m)*} \boldsymbol{a}(\theta))$ and locate the peaks.

5.2. A power-ESPRIT method

An approximated ESPRIT algorithm can be developed based on the following theorem.

Theorem 3. *Let E_1, E_2 be the matrices consisting of the first and last $p-1$ rows of the $p \times p$ identify matrix. Let S be as defined before and let E_q be a matrix such that $E_q^* U_s$ is nonsingular, then as $m \to \infty$, $(E_1 \hat{R}_x^m E_q)^+ E_2 \hat{R}_x^m E_q$ converges to a matrix which is similar to S. Here the notation A^+ denotes the Moore–Penrose inverse of A.*

Proof. See Appendix B. □

The matrix E_q in this theorem can be replaced by the selection matrix in Algorithm 2. In this case the limits

$$\lim_{m\to\infty} (E_1 Q_q^{(m)})^+ E_2 Q_q^{(m)} \tag{11a}$$

and

$$\lim_{m\to\infty} (E_1 C_q^{(m)})^+ E_2 C_q^{(m)} \tag{11b}$$

exist and the resulting matrices are similar to S.

6. Operation count

The methods presented in the previous sections are multiplication rich in that for a given m, $\hat{R}_x^m$ is required and followed by a matrix inversion. Matrix multiplication can be obtained very efficiently applying the Strassen algorithm [8]. In this algorithm, if $A \in R^{p\times p}$ and $B \in R^{p\times p}$ with p a power of 2, then $C = AB$ can be obtained with $s \approx p^{2.807}$ multiplications. Thus asymptotically, the number of multiplications in the Strassen algorithm is $O(P^{2.807})$ compared with $O(p^3)$ in the conventional method. It should be mentioned that in [1], Bailey implemented a Strassen approach that required only 60% of the time needed by the conventional multiplication.

The number of flops in computing $(b^m I_p - \hat{R}_x^m)^{-1}(b^m I_p + \hat{R}_x^m)$ consists of approximately the number of flops in computing $\hat{R}^m$ and the matrix inverse. Assuming that $m = 2^r$, both of these processes cost about $rp^{2.807} + \frac{2}{3}p^3$.

The number of flops required to compute the SVD of $\hat{R}_x$ by the Golub–Reinsch algorithm is $21p^3$ [7]. For example, if we choose r to be 4 which corresponds to $m = 16$, a value that is very high in most applications, the number of flops required in the rational MUSIC is $4p^{2.807} + \frac{2}{3}p^3$ which is still much less than $21p^3$ using the Golub–Reinsch algorithm [7].

Efficient matrix inversion can be computed using the LU decomposition. Once the LU factorization of A is known, the inverse matrix A^{-1} can be computed in $\frac{1}{3}p(p-1)(2p-1)$ flops [8]. Thus the total number of flops involved in computing $(b^m I_p - \hat{R}_x^m)^{-1}(b^m I_p + \hat{R}_x^m)$ is about $\frac{4}{3}p^3 + 2rp^3 = (2r + 1.333)p^3$. This number is still far less than the flop count for computing the SVD, which is about $21p^3$, for $r < 10$. Note that $r = 9$ corresponds to $m = 512$ which is extremely large for most applications. Thus for all practical purposes these algorithms which are based on Theorem 1 are less costly than the truncated SVD-based methods.

7. Implementation and numerical simulations

We present in this section several examples to illustrate the performance of the proposed algorithms. Based on Theorems 1–3, we have formulated several ways of approximating signal and noise subspaces. These approximations can be utilized to develop frequency estimators such as MIN-NORM, MUSIC and ESPRIT. It would be a very lengthy process to examine the performance of all these estimators. Thus we will only test the performance of Algorithms 1 and 2 for the MUSIC-type estimators and compare them with that of the truncated SVD-based method at SNR = 20, 15 and 10 dB and with different values of m. Several data sets consisting of two sinusoids were generated by the equation

$$x(n) = a_1 e^{j2\pi(f_1 n + \phi_1)} + a_2 e^{j2\pi(f_2 n + \phi_2)} + v(n), \tag{12}$$

where $a_1 = 1.0$, $a_2 = 1.0$, $f_1 = 0.5$, $f_2 = 0.52$, $n = 1, 2, \ldots, N = 25$, ϕ_1 and ϕ_2 are uniformly distributed over the interval [0 1]. The additive noise was colored and generated by passing a complex white Gaussian process of unit variance through an FIR filter with impulse response $\{1, 1, 1\}$. Note that $f_2 - f_1 < 1/N$. The SNR for either sinusoids is defined as $10\log_{10}(\sigma_s^2/\sigma_v^2)$, where $s(n) = a_1 e^{j2\pi(f_1 n + \phi_1)} + a_2 e^{j2\pi(f_2 n + \phi_2)}$ and σ_s^2, σ_v^2 are the variances of $s(n)$ and $v(n)$, respectively. The size of the sample covariance matrix is chosen to be $p = 10$ and is constructed using the forward-backward method described in Section 3, i.e., the matrix

$\hat{R}_x(0) = r_x(j, k)$, where

$$r_x(j, k) = \sum_{n=M}^{N-1} x^*(n-j)x(n-k) + \sum_{n=0}^{N-1-M} x(n+j)x^*(n+k), \quad j, k = 0, \dots, N-1. \tag{13}$$

The number M is chosen to be $M \geqslant p$. We will denote $\hat{R}_x(l) = [r_x(j+l, k+l)]$ which in case $l = 0$ represents an estimate of the covariance matrix of $x(n)$. Clearly in the absence of noise this matrix has effective rank two for each l. The SVD routine on MATLAB is used for the computation of the signal subspace eigenvectors and eigenvalues required to implement an SVD-based method for comparison. For each experiment (with data length and SNR fixed), we performed 100 independent trials to estimate the frequencies. We used the following performance criterion (RMSE):

$$\mathrm{RMSE} = \sqrt{\frac{1}{N_e} \sum_{i=1}^{N_e} (\hat{f}_i - f_{\mathrm{true}})^2},$$

to compare the results. Here N_e is the number of independent realizations, and $\hat{f}_i$ is the estimate provided from the ith realization. The SVD-based MUSIC is applied and the mean and RMSE obtained are shown in Table 2. The simulation results of applying Algorithms 1–2 and SVD-based MUSIC are summarized as follows.

1. *Algorithm 1.* The mean values and RMSE of the estimated frequencies are given in Table 1 for a set of 100 random experiments for different SNRs (SNR = 20, 15, 10 dB) using R_x^m with $m = 4$. The threshold b in these simulations is estimated by $b = \mathrm{Tr}(R_x)/p$. The peak spectrum was computed using 1000 frequency bins covering a normalized frequency range of 0 to 1. Also the peak spectrum is normalized so that its maximum equal to 1. The mean and RMSE are taken only over realizations where two peaks have occured. As can be noticed, the performance in these cases are almost identical to those obtained from using the exact decomposition. Fig. 1 shows the peaks resulted from applying Algorithm 1 for the case SNR = 15 dB with 30 realizations and using $R_x(10)^m$ for $m = 4$.

Table 1
Mean and RMSE of frequencies for data of two complex sinusoids at frequencies 0.50 and 0.52 in noise with SNR = 20, 15, 10 dB, dimension of data vector $p = 10$. Algorithm 1 is used with 100 realizations

SNR	f_1	f_2	RMSE_{f_1}	RMSE_{f_2}
20 dB	0.500732	0.520472	0.00641	0.016332
15 dB	0.500931	0.521788	0.00756	0.017123
10 dB	0.501183	0.525371	0.00963	0.022812

2. *Algorithm 2.* We repeated the experiments in part 1 using Algorithm 2. The results of testing this algorithm for different SNR are averaged over 100 trials and the mean and RMSE of each frequency is presented in Table 3. At SNR = 15 dB, it was estimated that the rate of joint detection of the two frequencies is identical to the SVD-based method. The signal subspace used was of dimension $q = 2$. As can be seen from Tables 2 and 3, the performance of Algorithm 2 is close to that of the standard MUSIC. Figs. 2 and 3 show the peaks resulted from applying Algorithm 2 and the standard MUSIC on 30 independent trials for the signals with SNR = 20 dB and using $R_x(10)^m$, $m = 4$.

We also performed experiments to explore the effect of the power m. It was observed that increasing m does not significantly affect the RMSE as long as $m \geqslant 3$ and $q = 2$.

Fig. 4 displays the spectrum distribution of 30 independent trials resulted from applying the three algorithms at SNR = 30 dB, $q = 2$ and $m = 4$. It is clear from the above tables and figures that the approximated methods and the standard MUSIC have almost identical performance especially at high SNR.

It should be pointed out that all the above results can be obtained with $m = 3$ but we used $m = 4$ to gain some computational saving by calculating R_x, R_x^2, R_x^4 using a squaring method. As can be seen, comparable results can still be obtained using low power $m = 4$ which indicates that the frequencies can be estimated at low computational cost.

When m is small it is also observed that overestimation of q leads to better estimation of the

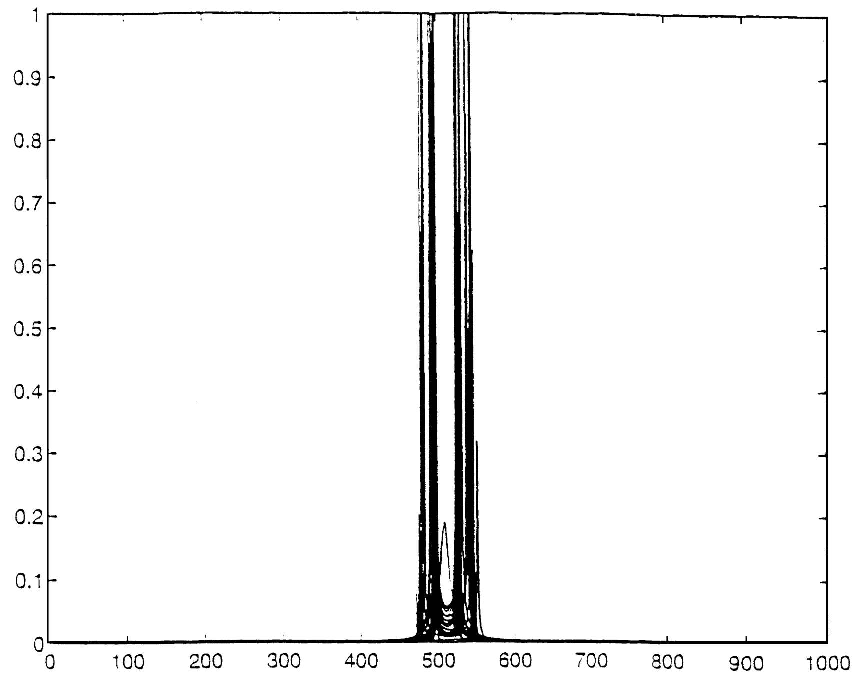

Fig. 1. Spectral distribution resulted from imposing the spectra of 30 independent trials at 15 dB using Algorithm 1 with $m = 4$.

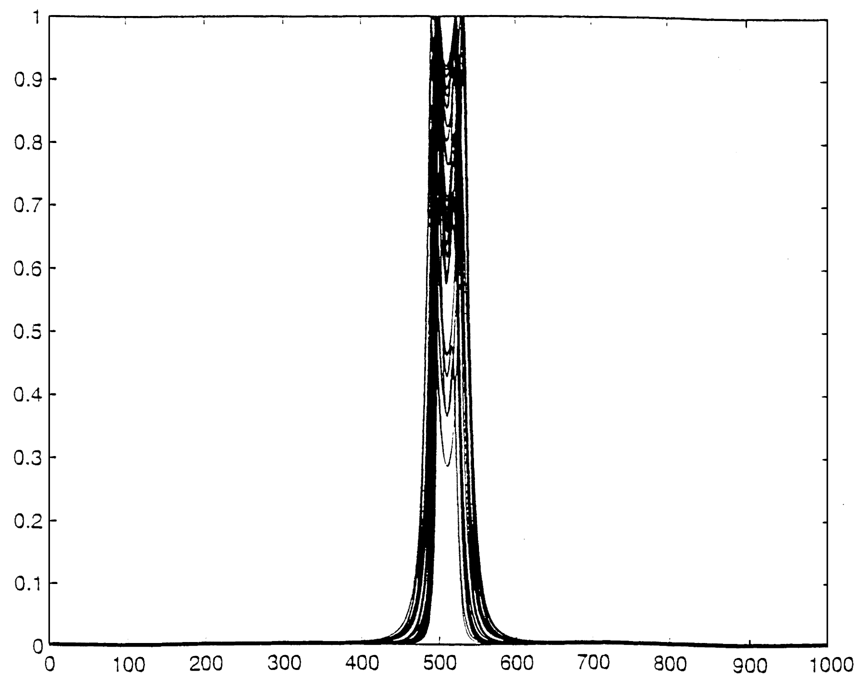

Fig. 2. Spectral distribution resulted from imposing the spectra of 30 independent trials at 20 dB using Algorithm 2, $q = 2$ and $m = 4$.

Table 2
Mean and RMSE of frequencies for data of two complex sinusoids at frequencies 0.50 and 0.52 in noise with SNR = 20, 15, 10 dB, dimension of data vector and signal subspace are $p = 10$ and $q = 2$, respectively. SVD-based method is used with 100 realizations

SNR	f_1	f_2	RMSE_{f_1}	RMSE_{f_2}
20 dB	0.50035	0.52174	0.00543	0.00597
15 dB	0.50093	0.52187	0.00942	0.00914
10 dB	0.50241	0.52274	0.01952	0.01473

Table 3
Mean and RMSE of frequencies for data of two complex sinusoids at frequencies 0.50 and 0.52 in noise with SNR = 20, 15, 10 dB, dimension of data vector are $p = 10$ and $q = 2$, respectively. Algorithm 2 is used with 100 realizations

SNR	f_1	f_2	RMSE_{f_1}	RMSE_{f_2}
20 dB	0.50126	0.52187	0.00784	0.00964
15 dB	0.50210	0.52251	0.00962	0.01883
10 dB	0.50271	0.52285	0.01927	0.02411

frequencies. The robustness of the methods against overestimation of the number of sources q can be explained as follows. Overestimation of q means additional vectors are included in the basis of the signal subspace. In our approximation, these vectors are not purely noise but contain some signal component. In the standard MUSIC, if an additional vector is added to the basis, a purely noise vector is included in the signal subspace causing spurious peaks.

8. Conclusion

In this paper, we have developed several approaches for approximating the signal subspace which avoid the costly eigendecomposition or SVD. It is shown that MUSIC, Minimum Norm and ESPRIT-type frequency estimators can be derived using these approximated subspaces. These approximate estimators are shown to be robust against noise and overestimation of

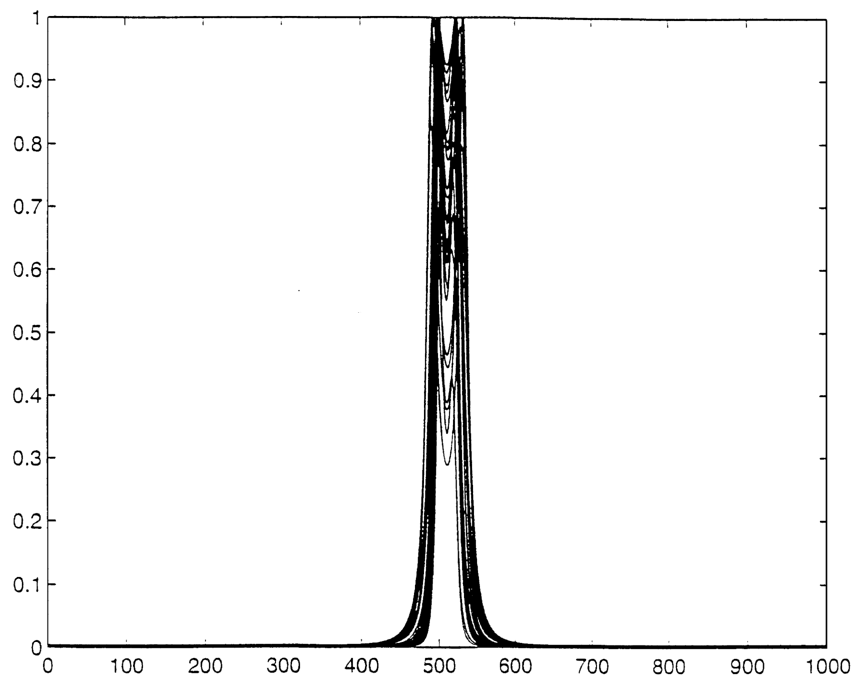

Fig. 3. Spectral distribution resulted from imposing the spectra of 30 independent trials at 20 dB using standard MUSIC with $q = 2$.

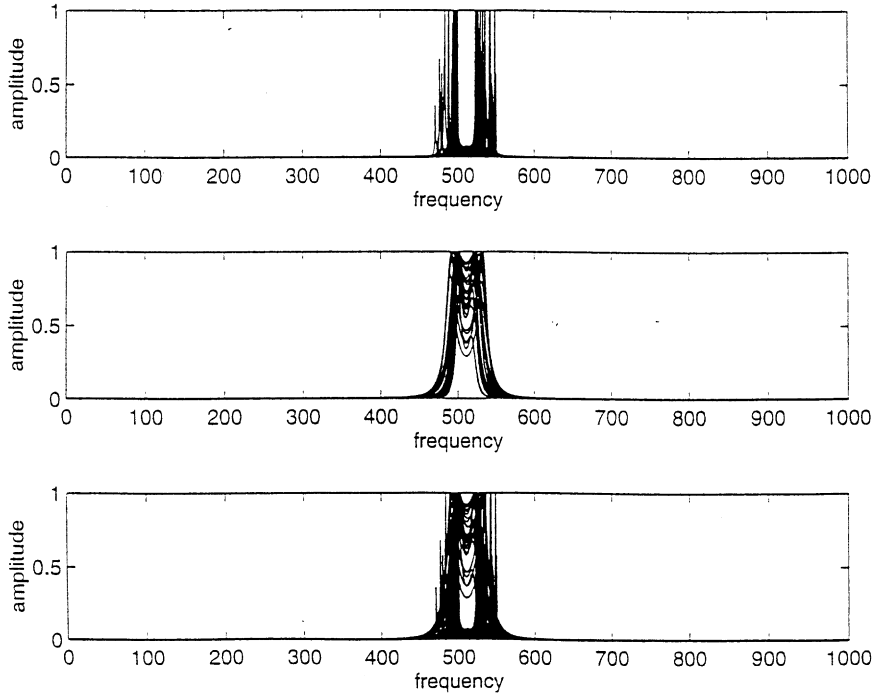

Fig. 4. Spectral peaks at $f_1 = 0.5$ and $f_2 = 0.52$ with SNR = 30 dB. The top, middle and bottom plots are obtained using Algorithm 1 with $m = 4$, the standard MUSIC with $q = 2$ and Algorithm 2 with $q = 2$ and $m = 4$, respectively.

number of sources. Even though these methods are introduced only as approximations, they perform well even at low SNR. The good performance of these approximate methods is due to the fact that the estimated signal and noise vectors obtained using the proposed algorithms are not purely signal or noise vectors, while methods based on exact eigendecomposition treat some of these vectors as purely signal or purely noise vectors which is not true especially at low SNR resulting in undesirable effects. We should mention that these methods are computationally simple in that only powers of the sample correlation matrix are required, Nonetheless, a comparable performance to high resolution exact eigenvector methods can be achieved using rational and power-type methods of approximating the signal subspace at a lower computational cost.

Finally, it should be stated that the performance of the proposed algorithms was not tested on more general signals having more than two sinusoids. This issue, among others, is being under consideration.

Acknowledgements

The author would like to thank the referees for their constructive comments which significantly improved the quality of this paper.

Appendix A. Proof of Theorem 1

From the eigendecomposition of $\hat{R}_x$, it follows that $(b^m I_p - \hat{R}_x^m)(b^m I_p + \hat{R}_x^m)^{-1} = \sum_{i=1}^{p} \frac{b^m - \lambda_i^m}{b^m + \lambda_i^m} \boldsymbol{u}_i \boldsymbol{u}_i^*$. To prove (1) we have (as $m \to \infty$)

$$\begin{aligned} &\frac{b^m - \lambda_i^m}{b^m + \lambda_i^m} \to -1, \quad \text{if } |b| < |\lambda_i|, \\ &\frac{b^m - \lambda_i^m}{b^m + \lambda_i^m} \to 1, \quad \text{if } |\lambda_i| < |b|. \end{aligned} \tag{A.1}$$

The rest of the conclusion of (1) follows from the fact that $U_nU_n^* + U_sU_s^* = I_p$. Similarly (2) follows from the observation that $\hat{R}_x^m(b^mI_p + \hat{R}_x^m)^{-1} = \sum_{i=1}^{p}(\lambda_i^m/(b^m+\lambda_i^m))\boldsymbol{u}_i\boldsymbol{u}_i^*$ and

$$\frac{\lambda_i^m}{b^m+\lambda_i^m} \to 1, \quad \text{if } |b| < |\lambda_i|,$$
$$\frac{\lambda_i^m}{(b^m+\lambda_i^m)} \to 0, \quad \text{if } |\lambda_i| < |b|. \tag{A.2}$$

The proof of (3) is analogous to that of (2) and follows directly from the identity $b^m(b^mI_p + \hat{R}_x^m)^{-1} = I_p - \hat{R}_x^m(b^mI_p + \hat{R}_x^m)^{-1}$. □

Appendix B. Proofs of Theorems 2 and 3

The proof of Theorems 2 and 3 follow directly from the following two results.

Lemma 1. *Let $A, C, B \in \mathscr{C}^{p\times p}$ be diagonalizable matrices such that $|\lambda_{\min}(A)| > |\lambda_{\max}(B)|$, then $(A^m)^{-1}CB^m \to 0$ as $m\to\infty$. ($\lambda_{\min}(A)$ and $\lambda_{\max}(A)$ denote the minimum and maximum eigenvalues of A.)*

Proof. We will only prove this lemma for diagonalizable matrices. Let $A = \sum_{i=1}^{p}\lambda_i\boldsymbol{q}_i\boldsymbol{p}_i^*$ and $B = \sum_{j=1}^{p}\mu_j\boldsymbol{u}_j\boldsymbol{v}_j^*$ with $\boldsymbol{p}_i^*\boldsymbol{q}_j = \boldsymbol{u}_j^*\boldsymbol{v}_j = \delta_{i-j}$. Then

$$(A^m)^{-1}CB^m = \left\{\sum_{i=1}^{p}\lambda_i^{-m}\boldsymbol{q}_i\boldsymbol{p}_i^*\right\}C\left\{\sum_{j=1}^{p}\mu_j^m\boldsymbol{u}_j\boldsymbol{v}_j^*\right\}$$
$$= \sum_{i=1}^{p}\sum_{j=1}^{p}\left(\frac{\mu_j}{\lambda_i}\right)^m\boldsymbol{q}_i\boldsymbol{p}_i^*C\boldsymbol{u}_j\boldsymbol{v}_j^*, \tag{B.1}$$

which converges to 0 since $|\mu_j| < |\lambda_i|$ for $i, j = 1, \ldots p$. □

The last result also holds for nondiagonalizable matrices and can be shown using a continuity argument.

Theorem 4. *Let $\hat{R}_x$ be a positive definite matrix such that $\hat{R}_x = Q\Lambda Q^*$, where $Q = \begin{bmatrix} Q_{11} & Q_{12} \\ Q_{21} & Q_{22}\end{bmatrix}$ is orthogonal matrix and $\Lambda = \begin{bmatrix}\Lambda_1 & 0 \\ 0 & \Lambda_2\end{bmatrix}$ is diagonal. Here Q_{11}, Q_{12}, Q_{21} and Q_{22} are $q\times q$, $q\times(p-q)$, $(p-q)\times q$ and $(p-q)\times(p-q)$ complex matrices, respectively. The matrices Λ_1 and Λ_2 are diagonal matrices such that $\Lambda_1 = \mathrm{diag}(\lambda_1,\ldots,\lambda_q)$ and $\Lambda_2 = \mathrm{diag}(\lambda_{q+1},\ldots,\lambda_q)$ with $|\lambda_{\min}(\Lambda_1)| > |\lambda_{\max}(\Lambda_2)|$. Assume without loss of generality that the matrix Q_{11} is nonsingular. Let $\hat{R}_x = \begin{bmatrix} R_{11} & R_{12} \\ R_{21} & R_{22}\end{bmatrix}$, and for each $m \geqslant 1$, let $\hat{R}_x^m = \begin{bmatrix} R_{11}(m) & R_{12}(m) \\ R_{21}(m) & R_{22}(m)\end{bmatrix}$, where R_{ij} and Q_{ij} have same dimensions, then*

$$\lim_{m\to\infty} R_{21}(m)R_{11}(m)^{-1} = Q_{21}Q_{11}^{-1} \tag{B.2}$$

and

$$\lim_{m\to\infty} R_{11}(m)^{-1}R_{12}(m) = Q_{11}^{-*}Q_{12}^*. \tag{B.3}$$

Proof. The decomposition

$$\hat{R}_x = \begin{bmatrix} Q_{11} & Q_{12} \\ Q_{21} & Q_{22}\end{bmatrix}\begin{bmatrix}\Lambda_1 & 0 \\ 0 & \Lambda_2\end{bmatrix}\begin{bmatrix} Q_{11} & Q_{12} \\ Q_{21} & Q_{22}\end{bmatrix}^* \tag{B.4}$$

is possible since $\hat{R}_x$ is Hermitian. From the relation (B.4) we obtain

$$\hat{R}_x^m = \begin{bmatrix} Q_{11} & Q_{12} \\ Q_{21} & Q_{22}\end{bmatrix}\begin{bmatrix}\Lambda_1^m & 0 \\ 0 & \Lambda_2^m\end{bmatrix}\begin{bmatrix} Q_{11} & Q_{12} \\ Q_{21} & Q_{22}\end{bmatrix}^* = \begin{bmatrix} Q_{11}\Lambda_1^mQ_{11}^* + Q_{12}\Lambda_2^mQ_{12}^* & Q_{11}\Lambda_1^mQ_{21}^* + Q_{12}\Lambda_2^mQ_{22}^* \\ Q_{21}\Lambda_1^mQ_{11}^* + Q_{22}\Lambda_2^mQ_{12}^* & Q_{21}\Lambda_1^mQ_{21}^* + Q_{22}\Lambda_2^mQ_{22}^*\end{bmatrix}.$$

Since $|\lambda_{\min}(\Lambda_1)| > |\lambda_{\max}(\Lambda_2)|$, it follows from Lemma 1 that

$$\lim_{m\to\infty} R_{21}(m)R_{11}(m)^{-1}$$
$$= \lim_{m\to\infty}(Q_{21}\Lambda_1^mQ_{11}^* + Q_{22}\Lambda_2^mQ_{12}^*)$$
$$\times(Q_{11}\Lambda_1^mQ_{11}^* + Q_{12}\Lambda_2^mQ_{12}^*)^{-1}$$

$$= \lim_{m\to\infty} (Q_{21}\Lambda_1^m Q_{11}^*)(Q_{11}\Lambda_1^m Q_{11}^*)^{-1}$$

$$= Q_{21}Q_{11}^{-1}.$$

Similarly, to prove Eq. (B.3) we have

$$\lim_{m\to\infty} R_{11}(m)^{-1}R_{12}(m)$$

$$= \lim_{m\to\infty} (Q_{11}\Lambda_1^m Q_{11}^* + Q_{12}\Lambda_2^m Q_{12}^*)^{-1}$$

$$\times (Q_{11}\Lambda_1^m Q_{21}^* + Q_{12}\Lambda_2^m Q_{22}^*)$$

$$= \lim_{m\to\infty} (Q_{11}\Lambda_1^m Q_{11}^*)^{-1}(Q_{11}\Lambda_1^m Q_{21}^*)$$

$$= Q_{11}^{*\,-1}Q_{12}^*. \quad \square$$

Proof of Theorem 2. Let $E_q = [W_1^T, W_2^T]^T$ with $W_1 \in \mathscr{C}^{q\times q}$ and $W_2 \in \mathscr{C}^{(p-q)\times q}$ such that $Q_{11}W_1$ is nonsingular and set $\hat{R}_x^m W = \begin{bmatrix} R_1(m) \\ R_2(m) \end{bmatrix}$, where $R_1(m) \in \mathscr{C}^{q\times q}$ and $R_2 \in \mathscr{C}^{(p-q)\times q}$. Then applying the same ideas of the proof of Theorem 4 we obtain

$$\lim_{m\to\infty} R_1(m)^{-1}R_2(m) = Q_{21}Q_{11}^{-1}.$$

By simple algebraic manipulation we obtain

$$\lim_{m\to\infty} \begin{bmatrix} R_1(m) \\ R_2(m) \end{bmatrix} (R_1^*(m)R_1(m) + R_2^*(m)R_2(m))^{-1}[R_1^*(m) \quad R_2^*(m)]$$

$$= \lim_{m\to\infty} \begin{bmatrix} R_1(m) \\ R_2(m) \end{bmatrix} \{R_1^{-1}(m)\{I_p + R_1^{-*}(m)R_2^*(m)R_2(m)R_1(m)^{-1}\}R_1(m)\}^{-1}[R_1^*(m) \quad R_2^*(m)]$$

$$= \lim_{m\to\infty} \begin{bmatrix} I_p \\ R_2(m)R_1^{-1}(m) \end{bmatrix} (I_p + R_1(m)^{-*}R_2^*R_2(m)R_1^{-1}(m))^{-1}[I_p \quad R_1^{-*}(m)R_2^*(m)]$$

$$= \begin{bmatrix} I_p \\ Q_{21}Q_{11}^{-1} \end{bmatrix} (I_p + Q_{11}^{-*}Q_{21}^*Q_{21}Q_{11}^{-1})^{-1}[I_p \quad Q_{11}^{-*}Q_{21}^*]$$

$$= \begin{bmatrix} Q_{11} \\ Q_{21} \end{bmatrix} (Q_{11}^*Q_{11} + Q_{21}^*Q_{21})^{-1}[Q_{11}^* \quad Q_{21}^*] = Q_1^*Q_1,$$

where $Q_1 = \begin{bmatrix} Q_{11} \\ Q_{21} \end{bmatrix}$ is defined in Theorem 4. Note that the third equality follows from Theorem 4. $\square$

Proof of Theorem 3. Since the columns of each of $A(\theta)$ and Q_1 span the signal subspace, it follows that $\begin{bmatrix} Q_{11} \\ Q_{21} \end{bmatrix} = A(\theta)P$ for some nonsingular matrix P. Therefore, for large m the matrix $\hat{R}_x^m W$ can be approximated as

$$\hat{R}_x^m W \approx \begin{bmatrix} Q_{11} \\ Q_{21} \end{bmatrix} \Lambda_1^m (Q_{11}^*W_1 + Q_{21}^*W_1) = Q_1\Lambda_1^m Q_1^* W$$

$$\approx A(\theta)P\Lambda_1^m Q_1^* W. \tag{B.5}$$

The nonsingularity of Q_1^*W guarantees that the matrix $R_1(m)$ is nonsingular for all sufficiently large m. Hence from Eq. (B.5) we also obtain

$$(E_2 R_x^m W)(E_1 R_x^m W)^+$$

$$\approx (E_2 A(\theta)P\Lambda_1^m Q_1^* W)(E_1 A(\theta)P\Lambda_1^m Q_1^* W)^+$$

$$= E_2 A(\theta)(E_1 A(\theta))^+,$$

which is similar to S. $\square$

Remark. One of the other important aspects of Theorem 4 is that the dominant eigenvectors can be extracted using only the elements of $\hat{R}_x^m$ for sufficiently large m. The only problem is that there is no guarantee that Q_{11} is invertible. This can be overcome by permuting the rows of $\hat{R}_x^m$. Another interpretation of Theorem 4 is that a basis of the signal subspace can be approximated by applying the Gram–Schmidt process on the columns of $\begin{bmatrix} I_p \\ R_{21}(m)R_{11}(m)^{-1} \end{bmatrix}$.

References

[1] D. Bailey, Extra high speed matrix multiplication on Cray-2, SIAM J. Sci. and Stat. Comp. 9 (1988) 603–607.

[2] K.M. Buckley, X-Liang Xu, Spatial spectrum estimation in a location sector, IEEE Trans. Signal Process. 38 (11) (November 1990) 1842–1852.

[3] A. Eriksson, P. Stoica, T. Soderstrom, Markov-based eigenanalysis method for frequency estimation, IEEE Trans. Signal Process. ASSP-42 (3) (March 1994) 586–594.

[4] V.T. Ermolaev, A.B. Gershman, Fast algorithm for minimum-norm direction of arrival estimation, IEEE Trans. Signal Process. 42 (9) (September 1994) 2389–2394.

[5] B.S. Garbow, J.M. Boyle, J.J. Dongarra, C.B. Moler, Matrix eigensystem routines-EISPACK guide extension, in: G. Goos, J. Hortmanis (Eds.), Springer, New York, 1977.

[6] A.B. Gershman, Direction of arrival estimation using generalized minimum norm approach, Electronics Letters 27 (16) (August 1991) 1485–1486.

[7] G.H. Golub, C. Reinsch, Singular value decomposition and least squares solutions, Numer. Math. 14 (1970) 403–420.

[8] G.H. Golub, C.G. Van Loan, Matrix Computations, 2nd edition, John Hopkins University Press, Baltimore, 1989.

[9] M. Haardt, J.A. Nossek, Unitary ESPRIT: How to obtain increased estimation accuracy with a reduced computational burden, IEEE Trans. Signal Process. ASSP-43 (May 1995) 1232–1242.

[10] M.A. Hasan, A.A. Hasan, Hankel matrices of finite rank with applications to signal processing and polynomials, J. of Math. Anal. and Appls. 208 (1997) 218–242.

[11] Y. Hua, T.K. Sarkar, On SVD for estimating generalized eigenvalues of singular matrix pencils in noise, IEEE Trans. Signal Process. 39 (4) (April 1991) 892–899.

[12] J.T. Karhunen, J. Joutsenalo, Sinusoidal frequency estimation by signal subspace approximation, IEEE Trans. Acoust. Speech Signal Process. ASSP-40 (12) (December 1992) 2961–2972.

[13] M. Kaveh, A.J. Barabell, The statistical performance of the MUSIC and minimum norm algorithms in resolving plane waves in noise, IEEE Trans. Acoust. Speech Signal Process. ASSP-34 (1986) 331–341.

[14] S.M. Kay, Modern Spectral Estimation, Theory and Applications, Prentice-Hall, Englewood Cliffs, NJ, 1988.

[15] S.M. Kay, A.K. Shaw, Frequency estimation by principal component AR spectral estimation method without eigendecomposition, IEEE Trans. Acoust. Speech Signal Process. 36 (1) (January 1988) 95–101.

[16] H.B. Lee, M.S. Wengrovitz, Resolution threshold of beamspace MUSIC for two closely spaced emitters, IEEE Trans. Signal Process. 38 (9) (September 1990) 1545–1559.

[17] H. Park, ESPRIT direction-of-arrival estimation in the presence of spatially correlated noise, SIAM J. Matrix Anal. Appl. 15 (1) (January 1994) 185–193.

[18] D.B. Rao, K.V.W. Hari, Performance analysis of root-music, IEEE Trans. Acoust. Speech Signal Process. 37 (12) (December 1989) 1939–1949.

[19] R.H. Roy, T. Kailath, ESPRIT-estimation of signal parameters via rotational invaiance techniques, IEEE Trans. Acoust. Speech Signal Process. ASSP-37 (7) (July 1989) 984–995.

[20] R.H. Roy, A. Paulraj, T. Kailath, ESPRIT-A subspace rotation approach to estimation of parameters of cisoids in noise, IEEE Trans. Acoust. Speech Signal Process. ASSP-34 (1986) 1340–1342.

[21] R.O. Schmidt, Multiple emitter location and signal parameter estimation, IEEE Trans. Acoust. Speech Signal Process. 34 (1986) 276–280.

[22] P. Stoica, T. Soderstrom, F. Ti, Asymptotic properties of the high-order Yule–Walker estimates of sinusoidal frequencies, IEEE Trans. Signal Process. 37 (11) (November 1989) 1721–1734.

[23] D. Tufts, C.D. Melissinos, Simple, effective computation of principal eigenvectors and their eigenvalues and application to high-resolution estimation of frequencies, IEEE Trans. Acoust. Speech Signal Process. 34 (5) (October 1986) 1046–1053.

[24] T.J. Ulrych, T.N. Bishop, Maximum entropy spectral analysis and autoregressive decomposition, Rev. Geophys. Space Phys. 13 (February 1975) 183–200.

[25] G. Xu, T. Kailath, Fast subspace decomposition, IEEE Trans. Signal Process. 42 (3) (March 1994) 539–551.